JOURNAL OF THE KOREAN ASTRONOMICAL SOCIETY
36: 97 ~ 103, 2003

COSMOLOGICAL APPLICATIONS OF MULTIPLY IMAGED GRAVITATIONAL LENS SYSTEMS

MYEONG-GU PARK
Department of Astronomy and Atmospheric Sciences, Kyungpook National University, Daegu 702-701, Korea
E-mail: mgp@knu.ac.kr
(Received April 30, 2003; Accepted August 17, 2003)

ABSTRACT

We now have more than 70 multiple image gravitational lens systems. Since gravitational lensing occurs through gravitational distortions in cosmic space, cosmological informations can be extracted from multiple image systems. Specifically, Hubble constant can be determined by the time delay measurement, curvature of the universe can be measured by the distribution of image separations in lens systems, and limits on matter density and cosmological constant can be set by the statistics of gravitational lens systems. Uncertainties, however, still exist in various steps, and results may be taken with some caution. Larger systematic survey and better understanding of galaxy properties would definitely help.

Key words : cosmology: observations — cosmology: miscellaneous — galaxies: general — gravitational lensing — quasars: general

I. INTRODUCTION

Gravitational lensing manifests itself in many different ways. It may produce multiple images, distort the image shapes prominently or subtly, change the image brightness, or modify the statistical characteristics of images. Among them, multiply imaged systems were the first observationally confirmed lensing cases and studied the most. In this talk, I will discuss how we can utilize these multiply imaged lens systems in study of cosmology.

II. OBSERVATIONAL STATUS

The first and best studied multiply imaged system is Q0957+561. It consists of two $z = 1.4$ QSOs, with $z = 0.36$ galaxy G1 and the surrounding cluster in between (Fig. 1). The fact that two images show the same spectral characteristics including the redshift, high-resolution VLBI map shows the radio morphology of the two images agree with theoretical expectation, and the time delay exists between the brightness variations of two images assures that Q0957+561 is a bona-fide gravitational lens system. Other multiple image QSO systems may or may not have similarly solid evidences. CASTLES (CfA-Arizona Space Telescope LEns Survey; http://cfa-www.harvard.edu/castles) provides the three grade of likelihood that a given multiple image system is gravitationally lensed one: "A" for "I'd bet my life.", "B" for "I'd bet your life.", and "C" for "I'd bet your life and you should worry.". CASTLES currently lists 72 multiple image lens systems. Among them, 54 are "A-grade", 9 are "B-grade", and 9 are "C-grade" lens systems.

III. INFORMATION

Generally usable information from observed multiply imaged lens systems are the total number of images, redshifts of the source and lens, positions of images and lens, the brightness ratios between images, and time delays between images. Though it sometimes is not trivial to count the total number of images due to merged or faint images, the number of images in general range from 2 up to 10: 44 are two image cases, 19 are four image cases, single case for five and six image system. Even ten image system exists (B1933+507). The remaining cases are ring systems.

Although the number of images and brightness ratios between them are very important constraints when building a specific lens model, they have been less widely exploited in cosmological applications than the statistical properties of lens systems. Redshifts of sources, z_s, range from 0.96 (B0218+357) to 4.12 (PSS2322+1944) while those of lens galaxies, z_l, range from 0.04 (Q2237+030) to 1.01 (MG2016+112). The characteristics of a certain cosmological model affects the expected properties of lens systems through the relation between the redshift and the angular (or luminosity) distance. For example, highly curved cosmological model and flat cosmological model give different angular distances for the same redshift, and thereby producing different image separations. The relative positions of images and lens are also critical information while building model for specific lens case, yet hard to implement in the statistical studies. Separations between images, the maximum separation among images or average separations, are more commonly used in cos-

Proceedings of the APCTP Workshop on *Formation and Interaction of Galaxies*

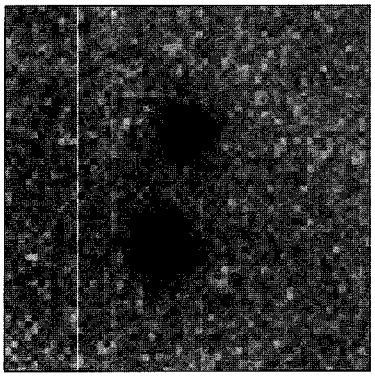

Fig. 1.— Doubly imaged gravitational lens system Q0957+561. Top image is A and bottom one B.

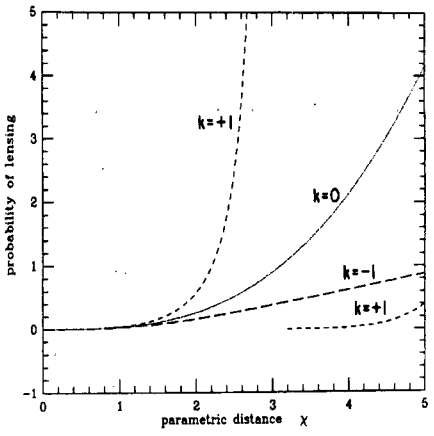

Fig. 2.— Probability of multiple image lensing in universes with different curvature k as a function of parametric distance χ.

mological applications. Time delay between different images also provide invaluable cosmological information.

IV. THE HUBBLE CONSTANT H_0

Well before the actual discovery of multiple image gravitational lens systems, Sjur Refsdal realized that if brightness of the source quasar fluctuates, the fluctuation would appear in each image at different times (Refsdal 1964). This difference in time is called time delay, the magnitude of which would depend on the difference in light paths as well as on the "effective" speed of light in gravitational potential well. Therefore, if the gravitational potential of the lens is known by some other means, the whole scale of lens geometry can be fixed by the measurement of time delay. Since the whole geometrical scale of cosmological lensing is inversely proportional to the Hubble constant, the Hubble constant can be determined from the measured value of time delay:

$$\begin{aligned} \text{Time delay} \;\simeq\; & h^{-1} \times 1 \text{ month} \\ & \times \text{ image separation in arcsec} \\ & \times (1 + z_{lens}) \\ & \times \text{ weak dependence on } z_{lens},\ z_{QSO}, \\ & \quad \text{and cosmology} \\ & \times \text{ lens mass distribution-dependent} \\ & \quad \text{factor,} \end{aligned}$$

where h is H_0 in units of 100 km s^{-1} Mpc^{-1}, z_{lens} and z_{QSO} are the redshifts of lens and QSOs, respectively.

Again, the best studied lens system with measured time delay is Q0957+561. High precision photometry from December 1994 to July 1996 show good match between light curve of image A, shifted 418 days, and that of image B (Kundić et al. 1997). Combining this time delay with a specific model of mass distribution in lens produces an estimate $H_0 = 64 \pm 13$ km s^{-1} Mpc^{-1}. Other systems including radio lens systems also have time delays measured. See table 1 for details.

Table 1. Measured Time Delay

Lens System	z_{source}	z_{lens}	Δ_t (days)
B0218+357[1] B/A	0.96	0.68	10.5 ± 0.4
Q0957+561[2] B/A	1.41	0.36	417 ± 3
PG1115+080[3,4] C/B	1.72	0.31	$25.0^{+3.3}_{-3.8}$
B1600+434[5] B/A	1.59	0.42	47 ± 6
B1608+656[6] C/B	0.63	1.39	$31.5^{+2.0}_{-1.0}$
B1608+656[6] A/B			$36.0^{+1.5}_{-1.5}$
B1608+656[6] D/B			$77.0^{+2.0}_{-1.0}$
PKS1830-211[7] B/A	2.51	0.89	26 ± 5

References—(1) Biggs et al. 1999; (2) Kundić et al. 1997; (3) Schechter et al. 1997; (4) Barkana 1997; (5) Burud et al. 2000; (6) Fassnacht et al. 2002; (7) Lovell et al. 1998

Estimate of Hubble constant H_0 from the time delay measurement ranges from 50 $\sim$ 70 km s^{-1} Mpc^{-1}. Determining H_0 this way is completely skips the usual distance ladder, and therefore quite complementary to the conventional method to determine H_0. The main limitations in this method, however, is the incomplete knowledge of lens potentials, or equally, mass distribution. Uncertainties in the model of lens potential introduces significant errors to the estimate. Improving the estimate, therefore, requires accurate mapping of mass distribution of lens. With bigger telescopes, better detectors and space observations, positions and light distributions of lensed images, lensing and surrounding

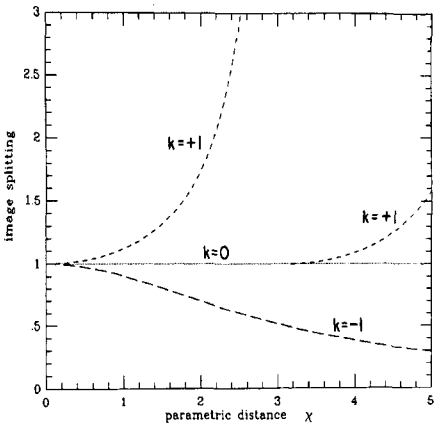

Fig. 3.— Mean angular separation between images in universes with different curvature k as a function of parametric distance χ.

galaxies are better mapped. Additional spectroscopic observations will also help to fix the mass distribution. All these improvements will ultimately lead to secure determination of Hubble constant from lens time delay alone.

V. CURVATURE OF THE UNIVERSE

Shape of the cosmic space fundamentally affects the lensing geometry. For example, given the same lensing geometry, i.e., the same redshifts for source and lens and the same lens mass distribution, the probability of multiple image lensing and the separation angle between images are different for different cosmological models (TOG).

Combining a simple model for the lens mass distribution, e.g., singular isothermal sphere, with a spatial distribution, e.g., homogeneous distribution in comoving space, the probability of lensing and statistical properties of image separation can be calculated (GPL).

For the same parametric distance, the probability of lensing (see Fig. 2) is highest for positively curved space ($k = +1$) and lowest for negatively curved space ($k = -1$). So is the angular image separation (see Fig. 3). Positively curved space acts like a cosmic magnifier. This is in a way collective effect of matter in the universe that curves the space as it is. Hence, gravitational lensing in cosmic scale is the sum of lensing by the lensing galaxy and the universe itself.

Also notable is that the mean image separations is constant in a flat universe as a function of source redshift, regardless of the cosmological constant (see Fig. 3). This means the curvature of the universe can be tested with multiple image lens systems by comparing the expected mean image separation with the image separations observed in real lens systems. This

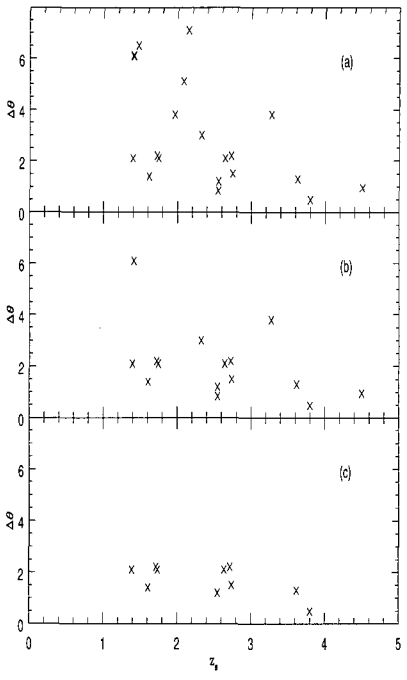

Fig. 4.— Mean angular separation between images in universes with different curvature k as a function of parametric distance χ.

test was performed in 1989 with small number of then-available lens cases (GPL). Though the test could not discern among generally explored cosmological models, extreme $k = +1$ cosmological models, e.g., very large cosmological constant models, could be ruled out. This test was redone in 1997, but the maximum image separation from 20 lens cases show strong decrease as redshift of the source increases (see Fig. 4a). This is not consistent with any FLRW cosmological models including the empty universe model (Park & Gott 1997). It may be the result of unknown observational selection effects, unusual galaxy properties (Williams 1997) or unfair sample of lens cases employed (Khare 2001), though this is not at all clear at the moment. It is even suggested that most of lens systems with large separation may not be real gravitational lens systems but binary QSOs (Kochanek et al. 1999). Whatever the real answer be, this illustrates the uncertainties involved in cosmological tests using finite sample of lens cases.

Now, let's ask how many multiple image lens cases are needed to meaningfully determine the curvature of the universe. If we assume that, among the lens systems used by Park & Gott (1997), only those with image separation less than 4" and Q0957+561 are genuine (see Fig. 4b) , that it is not distorted by unknown selection effect and that all to-be-discovered lens systems follow the same scattered distribution, 450 lens sys-

tems are required to distinguish the flat universe versus empty universe. Proving or disproving a less extreme open universe like the $\Omega_0 = 0.4$, $\Omega_\Lambda = 0$ universe at the same 95% confidence level requires 900 cases. It won't be easy, but is certainly possible. On the other hand, if future lens systems follow the narrow distribution of Kochanek (1996) sample (see Fig. 4c), only 130 lens systems are needed to test the empty universe and 280 systems to test the $\Omega_0 = 0.4$, $\Omega_\Lambda = 0$ open universe.

VI. Ω_0 AND Ω_Λ

(a) Overfocusing of QSO beyond the Antipode

There are other ways to infer cosmological information from multiple image lensing. Gott, Park & Lee (1989) explored the lensing in closed universe with an antipode. They found that if the source, e.g. QSO, is located beyond the antipode, overfocusing occurs and only one arbitrarily dim image coincident with the position of the lensing galaxy center is seen where as in normally lensed case two or more images occur. This remains true even if the galaxy has an elliptical potential or if there is an additional quadrupole tidal field without excessive shear. So if we observe a normal lensed cases consisting of bright double images with the lensing galaxy located roughly between them, the source cannot be beyond the antipode. Therefore, the existence of normal lensing cases at a given redshift constraints the antipodal redshift to be higher than the redshift of the source. The lens system BRI 0952-0115 has so far the highest source redshfift of $z_s = 4.5$ and is very likely to be a normal lensing case. This limit on antipodal redshfift ($z_{antipode} > 4.5$) excludes certain part of (Ω_0, Ω_Λ) parameter space (diagonally shaded part in Fig. 5). The horizontally shaded region is no big bang region.

(b) Probability of Lensing Test

Although Gott, Park & Lee (1989) calculated the lensing probability for universe with arbitrary Ω_Λ, it was Fukugita & Turner (1991) who tested the expected probability against the actual number of lens cases found. They recognized the fact that the number of multiple image lens cases sharply increases as Ω_Λ increases. Hence, if we live in a universe with large Ω_Λ, we should have discovered many times more multiple image lens cases than we actually have discovered so far. This discrepancy implies that we don't live in Ω_Λ-dominated universe. Fukugita & Turner concludes that $\Omega_\Lambda < 0.9$.

(c) Maximum Likelihood Test

Kochanek (1996) extended this type of test to utilize additional information like image separation and magnitude as well as the number of lens cases. He used the maximum likelihood method: For each given (Ω_0,Ω_Λ) universe model, he calculated the likelihood that the

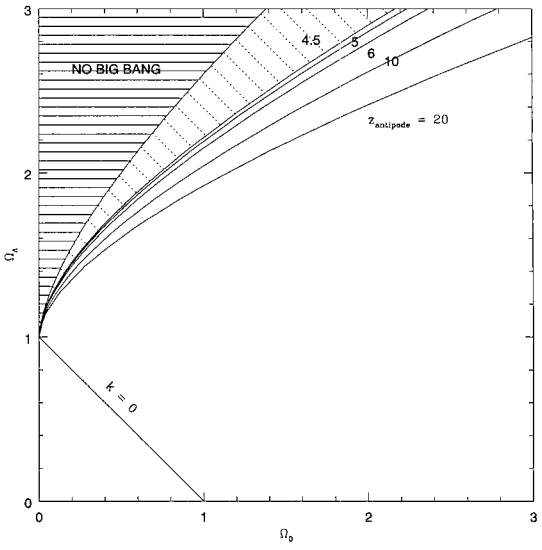

Fig. 5.— The lines of constant antipodal redshift in Ω_0 versus Ω_Λ plane. The horizontally and diagonally shaded regions are both excluded if $z_{antipode} > 4.5$. The solid line $k = 0$ represents the flat universe ($\Omega_0 + \Omega_\Lambda = 1$.

expected number of lens cases and their image configurations actually match those observed, yielding limits on Ω_Λ using quasar surveys, lens data and a range of lens models. The formal limits were $\Omega_\Lambda < 0.66$ at 95% confidence in flat cosmologies ($\Omega_0 + \Omega_\Lambda = 1$) and $\Omega_0 > 0.15$ in open universes with $\Omega_\Lambda = 0$, including the statistical uncertainties in the number of lenses, galaxies, and quasars and the parameters relating galaxy luminosities to dynamical variables. He also mentions that although extinction in early type galaxies can significantly alter the limits on Ω_Λ, changing the expected number of lenses by a factor of 2 would require more than 100 times the extinction seen locally in early type galaxies.

Helbig et al. (1999) repeated this test with Jodrell Bank-VLA Astrometric Survey (JVAS) radio data. Although JVAS is the largest gravitational lens survey, the redshifts of sources in radio surveys are typically lower than the optical surveys and the luminosity function of radio sources as a function of redshift is less well known compared to the optical quasars. JVAS lensing statistics alone limits with 95% confidence $\Omega_\Lambda - \Omega_0$ to be in the range -2.69 to 0.68 (Helbig et al. 1999). Figure 6 shows the likelihood contours from JVAS lensing statistics in (Ω_0,Ω_Λ) parameter space. For flat cosmological models, the limits corresponds to $-0.39 < \Omega_\Lambda < 0.64$, consistent with the limits of Kochanek (1996). The model with maximum likelihood, however, is Ω_Λ-dominated one, near $\Omega_\Lambda = 0.5$, in contrast with previous lensing statistics result, in which $\Omega_\Lambda = 0$ models were most preferrable (Fukugita & Turner 1991; Kochanek 1996).

Interestingly, when the statistics of images separations alone are used to check flat models , models with

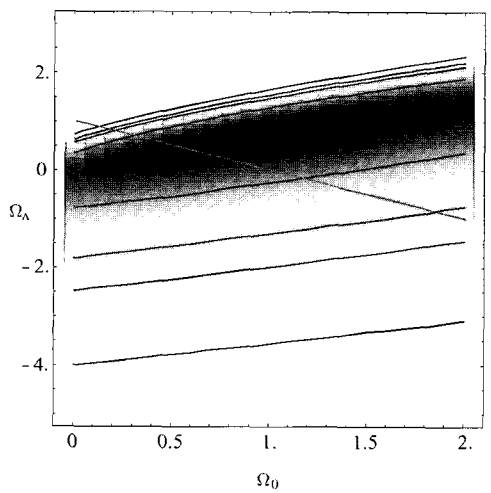

Fig. 6.— The likelihood map based on JVAS sample. The pixel gray level is directly proportional to the likelihood ratio, darker pixels being higher ratios. The contours mark the boundaries of the minimum 0.68, 0.90, 0.95 and 0.99 confidence regions for the parameters Ω_0 and Ω_Λ. The gray diagonal line represents flat ($\Omega_0 + \Omega_\Lambda = 1$) models. (Helbig 1999; astro-ph/9901175)
]vskip -0.4cm

large Ω_Λ are preferred. Lee & Park (1994) used observed redshifts of both lens and source as well as image separations to compare with the expected distribution of image separation for given lens and source redshifts. Statistical analyses showed that flat models with larger Ω_Λ were preferred although $\Omega_\Lambda = 0$ were not ruled out with enough confidence. Park (1996) tested "standard" lensing statistics model, singular isothermal sphere galaxy in flat universe, against the distribution of image separations (summed over all redshifts) in observed lens systems. The observed distribution seemed inconsistent with the expected one, but the confidence of rejection was not high enough except the radio lens cases. Also, test results were dependent on lens samples and angular selection functions.

Current larger and better lens survey like HST Snapshot Survey (HST) and Jodrell Bank-VLA Astrometric Survey/Cosmic Lens All Sky Survey (JVAS/CLASS) now yield much stronger result (Lee & Park 2003). Exactly which lens cases are included in the sample and what galaxy parameters are used determines the test result. Figure 7 shows the likelihood contours of lens image separation statistics for HST (bottom row in Fig. 7), for JVAS/CLASS (middle row) and for HST/CLASS (top row). Each column is for different choice of galaxy parameters, e.g., power index and characteristic velocity dispersion in Schechter luminosity function. Leftmost column for parameters determined from Las Campanas galaxy survey, second left from APM survey, third left from CfA survey and the rightmost from those used in Fukugita et al. (1992, FFKT). Although they all show different contours, the general trend is quite clear. Region near $\Omega_0 = 0$, $\Omega_\Lambda = 1$ has the greatest likelihood. If limited to flat models, Ω_Λ close to 1 models are more likely and $\Omega_\Lambda = 0$ models are almost always ruled out with more than 95% confidence.

These results from the statistics of image separations agree rather well with recent constraints from the magnitude-redshift relations of Type Ia supernovae discovered in Supernova Cosmology Project (Perlmutter et al. 1999) and High-Z Supernova Search Team (Riess et al. 1998). Figure 8 is the same gray scale contour map of likelihood from SCP data (Perlmutter et al. 1999; Helbig et al. 1999). Higher Ω_Λ models have higher likelihood and $\Omega_\Lambda \simeq 0.7$, $\Omega_0 \simeq 0.3$ model is most likely among flat models.

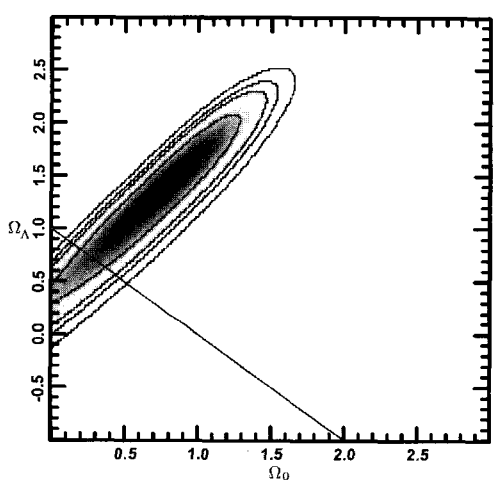

Fig. 8.— The likelihood map from Type Ia supernova magnitude-redshift relations (Perlmutter et al. 1999; Helbig et al. 1999).

Apparently, testing cosmological models with the probability of lensing yields different result than with statistics of image separations. It is common belief that image separations are less sensitive to cosmological models than the number of lens cases. However, calculating the expected number of multiple image lens cases can be quite daunting, considering our ignorance in galaxy luminosity function as a function of redshift, quasar luminosity function also as a function of redshift, magnification bias and so forth. It is even more difficult for radio lenses. It is not clear, however, at the moment which one of above is the exact cause of the discrepancies. Suffice it to say that applying lens statistics to test cosmological models needs extra cautions, and confirmation by different type of lens statistics is desirable.

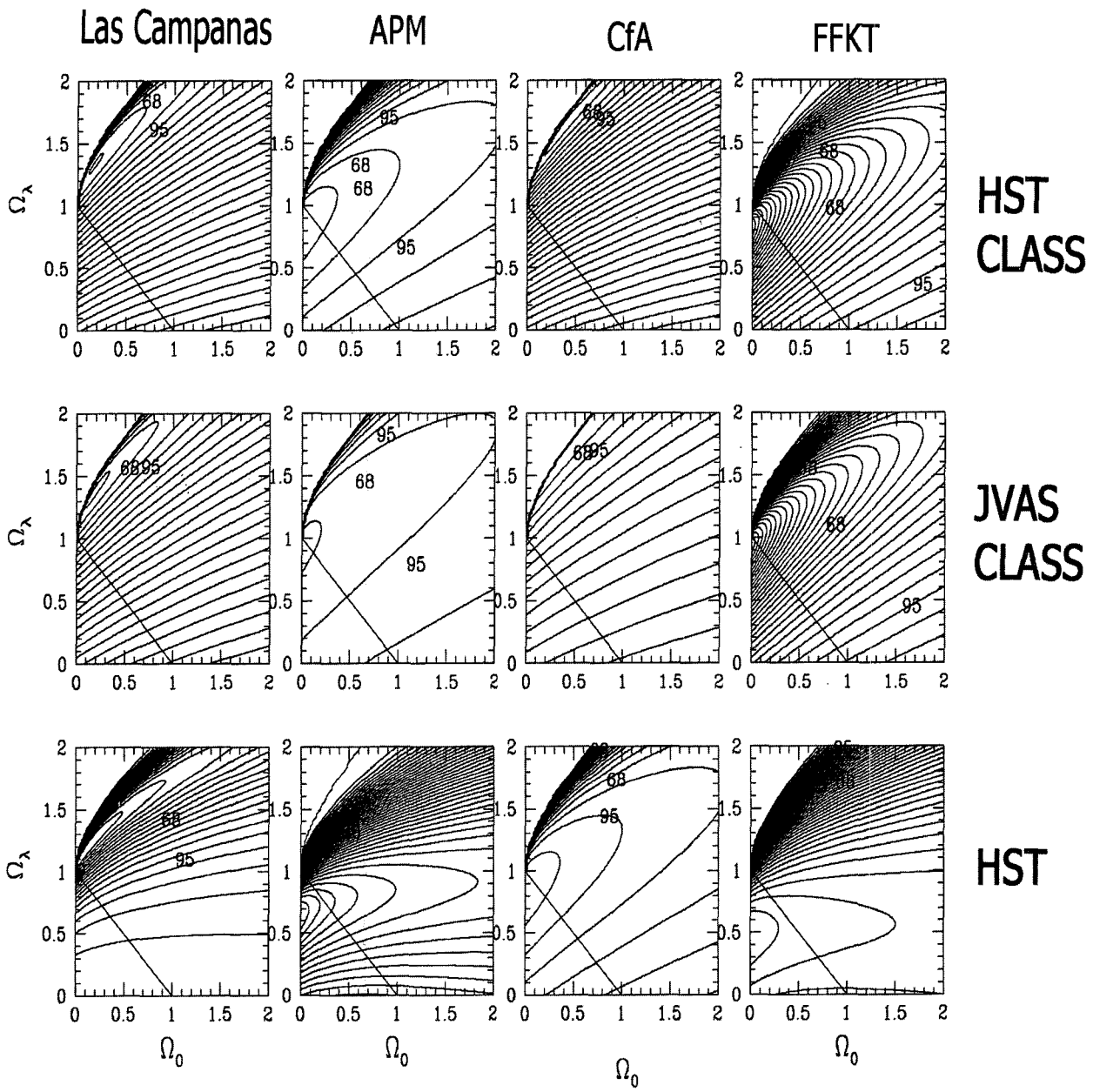

Fig. 7.— The likelihood contours for HST, JVAS/CLASS and HST+CLASS surveys and for galaxy parameters from Las Campanas, APM, CfA and FFKT. The diagonal line represents flat models and numbers 68 and 95 mark the boundaries of 68% and 95% confidence regions, respectively.

VII. CONCLUSION

Multiple image gravitational lens system can be a very useful tool to determine cosmological parameters and to test various cosmological models. Uncertainties, however, still exist in various steps, and results may be taken with some caution. Larger systematic survey and better understanding of galaxy properties would definitely help.

This work was supported by grant No. R01-1999-00023 from the Korea Science & Engineering Foundation.

REFERENCES

Barkana, R. 1997, Analysis of Time Delays in the Gravitational Lens PG 1115+080, ApJ, 489, 21

Biggs, A. D., Browne, I. W. A., Helbig, P., Koopmans, L. V. E., Wilkinson, P. N., & Perley, R. A. 1999, Time Delay for the Gravitational Lens System B0218+357, MNRAS, 304, 349

Burud et al. 2000, An Optical Time Delay Estimate for the Double Gravitational Lens System B1600+434, ApJ, 544, 117

Fassnacht, C. D., Xanthopoulos, E., Koopmans, L. V. E., & Rusin, D. 2002, A Determination of H0 with the Class Gravitational Lens B1608+656. III. A Significant Improvement in the Precision of the Time Delay Measurements, ApJ, 581, 823

Fukugita, M., Futamase, T., Kasai, M. & Turner, E. L. 1992, Statistical Properties of Gravitational Lenses with a Nonzero Cosmological Constant, ApJ, 393, 3

Gott, J. R., Park, M.-G. & H. M. Lee 1989, Setting Limits on q_0 from Gravitational Lensing, ApJ, 338, 1

Helbig, P., Marlow, D. R., Quast, R., et al. 1999, Gravitational Lensing Statistics with Extragalactic Surveys: II. Analysis of Jodrell Bank-VLA Astrometic Survey, A&AS, 136, 297

Khare, P. 2001, Angular Separations of Lensed Quasar Images, ApJ, 550, 153

Kochanek, C. S., Falco, E. E., & Muñoz, J. A. 1999, Why Quasar Pairs are Binary Quasars and Not Gravitational Lenses, ApJ, 510, 590

Kochanek, C. S. 1996, Is There a Cosmological Constant?, ApJ, 466, 638

Kundić, T., et al. 1997, A Robust Determination of the Time Delay In 0957+561A, B and a Measurement of the Global Value of Hubble's Constant, ApJ, 482, 75

Lee, H.-A & Park, M.-G. 1994, Statistical Properties of Gravitational Lensing in Cosmological Models with Cosmological Constant, JKAS, 27, 103

Lee, H.-A & Park, M.-G. 2003, *in preparation*

Lovell, J. E. J., et al. 1998, The Time Delay in the Gravitational Lens PKS 1830-211, ApJ, 508, L51

Park, M.-G. 1996, Gravitational Lensing Statistics in a Flat Universe, JKPS, 29, 664

Park, M.-G. & Gott, J. R. 1997, Curvature of The Universe and Observed Gravitational Lens Image Separations versus Redshift, ApJ, 489, 476

Perlmutter S., Aldering G., Goldhaber G., et al., 1999, Measurements of Omega and Lambda from 42 High-Redshift Supernovae, ApJ 517, 565

Refsdal, S., 1964, On the possibility of determining Hubble's parameter and the masses of galaxies from the gravitational lens effect, MNRAS, 128, 307

Riess A.G., Filippenko A.V., Challis P., et al., 1998, Observational Evidence from Supernovae for an Accelerating Universe and a Cosmological Constant, AJ 116, 1009

Schechter, P. L., et al. 1997, The Quadruple Gravitational Lens PG 1115+080: Time Delays and Models, ApJ, 475, L85

Williams, L. L. R. 1997, Image Separation versus Redshift of Lensed QSOs - Implications for Galaxy Mass Profiles, MNRAS, 292, L27